Theoretical predictions of alkali hexazirconate ($A_2Zr_6O_{13}$, A= Li, Na, and K) as candidates for alkali ion batteries

Predicciones teóricas de hexazirconatos alcalinos ($A_2Zr_6O_{13}$, A= Li, Na y K) como candidatos para baterías de iones alcalinos

J.R. Fernández-Gamboa,[1*] https://orcid.org/0000-0001-5069-5240
Yohandys A. Zulueta,[1] https://orcid.org/ 0000-0003-0491-5817
My Phuong Pham-Ho[2], https://orcid.org/0000-0002-8874-0163
Frederick Tielens,[3] https://orcid.org/0000-0002-6760-6176
Minh Tho Nguyen[4] ,https://orcid.org/ 0000-0002-3803-0569

[1] Departamento de Física, Facultad de Ciencias Naturales y Exactas, Universidad de Oriente, Santiago de Cuba, Cuba
[2] Faculty of Chemical Engineering, Ho Chi Minh City University of Technology (HCMUT), Vietnam
[3] General Chemistry (ALGC)–Materials Modelling Group, Vrije Universiteit Brussel, Belgium.
[4] Laboratory for Chemical Computation and Modeling, Institute for Computational Science and Artificial Intelligence, Van Lang University, Vietnam

[*]Corresponding author: jrfernandez@uo.edu.cu

ABSTRACT

The complete transition to renewable energy sources is limited by your intermittent energy generation. The battery provides the portability of stored chemical energy with the ability to deliver this energy as electrical energy with a high conversion efficiency. The oxide based on the Andersson-Wadsley family has received increasing attention to use as an anode of battery due to this structure presenting the tunnel to ionic transport. The structural, electronic, and mechanical properties of $Li_2Zr_6O_{13}$ and unknown materials $Na_2Zr_6O_{13}$ and $K_2Zr_6O_{13}$ were evaluated using classical simulations and DFT calculations. The electronic band structure analysis points out the insulator character of $Li_2Zr_6O_{13}$ and $Na_2Zr_6O_{13}$ and the semiconductor character of the $K_2Zr_6O_{13}$ compound. The reaction ion exchange of Li/K, Li/Na, and K/Na is energetically favourable to the synthesis of the unknown materials $K_2Zr_6O_{13}$ and $Na_2Zr_6O_{13}$,

respectively, for this reason, these compounds can be recommended as an alternative material for energy storage in ion-batteries.
Keywords: alkali-Ion Battery; atomistic simulations; structural properties; band gap.

RESUMEN

La transición completa a fuentes de energía renovable está limitada por su generación de energía intermitente. La batería proporciona la portabilidad de la energía química almacenada con la capacidad de entregarla como energía eléctrica con una alta eficiencia de conversión. Los óxidos basados en la familia Andersson-Wadsley han recibido una creciente atención en su uso como ánodo de batería, debido a que presenta una estructura tipo túnel que favorece el transporte iónico. Las propiedades estructurales, electrónicas y mecánicas del $Li_2Zr_6O_{13}$ y de los materiales desconocidos $Na_2Zr_6O_{13}$ y $K_2Zr_6O_{13}$ se evaluaron mediante simulaciones clásicas y cálculos DFT. El análisis de la estructura de banda electrónica señala el carácter aislante de $Li_2Zr_6O_{13}$ y $Na_2Zr_6O_{13}$ y el carácter semiconductor del $K_2Zr_6O_{13}$. La reacción de intercambio iónico de Li/K, Li/Na y K/Na es energéticamente favorable para la síntesis de los materiales desconocidos $K_2Zr_6O_{13}$ y $Na_2Zr_6O_{13}$, respectivamente, por lo que estos compuestos pueden recomendarse como material alternativo para el almacenamiento de energía en baterías de iones.
Palabras clave: batería de iones alcalinos; simulaciones atomísticas; propiedades estructurales; band pap.

Recibido: 15/6/2023

Aprobado: 30/7/2023

Introduction

It is now almost universally recognized that gaseous emissions from the burning of fossil fuels and biomass are not only polluting the air of large, modern cities but are also creating global warming with alarming consequences. Moreover, dependence on foreign oil and/or gas creates national vulnerabilities that endanger social stability. These concerns are concentrating attention once again on national initiatives to evaluate the utilization of alternative energy sources and the replacement of the internal combustion engine with a wireless electric motor. However, the complete transition to renewable energy sources is

limited by your intermittent energy generation. The battery provides the portability of stored chemical energy with the ability to deliver this energy as electrical energy with a high conversion efficiency and no gaseous exhaust. Whereas alternative energy sources are stationary, which allows other means of energy storage to be competitive with a battery, electric vehicles require the portable stored energy of a fuel fed to a fuel cell or of a battery. High specific energy density and capacity, high cycle lifetime, and fast charge capabilities are the main goals that lithium batteries have to reach to jump from portable devices to hybrid or electric vehicles. Such a large-scale market demand will sustain an important research activity on the development of new battery configurations and hence new battery chemistries.[1-4]

Titanium oxide-based materials have been intensively investigated because of their potential applications as electrodes for lithium-ion batteries, photocatalysts, or semiconductor devices. More recently, the alkali metal titanate family with the general chemical formula $A_2Ti_6O_{13}$ (A = Na, Li, K, H) has awakened much interest due to a wide range of interesting chemical properties.[5-9]

Among several types of technologically important oxides, those based on the Andersson-Wadsley family ($A_2O{\cdot}nTiO_2$; A = alkali cation; $1 \leq n \leq 6$) have received increasing attention. The n = 6 members, i.e., alkali hexatitanate $A_2Ti_6O_{13}$, have been extensively studied for several potential applications.[5,10,11] Three [TiO_6] octahedra are edge-shared in a row forming a building block, and the block is connected with identical blocks above as well as below resulting in a ribbon. The ribbons are corner-shared, resulting in an $[Ti_6O_{13}]^{2-}$ framework with the tunnel extending along the b-direction. Based on symmetries, there are seven types of oxygen atoms in this structure with a coordination number ranging from 2 to 4. The larger K^+ and Na^+ cations coordinate to eight oxygen atoms in a distorted tetragonal prism [(K/Na)O_8]. On the contrary, the smaller Li^+ cations form a distorted [LiO_3] triangular geometry.[5,7,10,11] In general, alkali hexatitanate compounds have a tunnel structure that allows for the accommodation and migration of alkali ions. $Li_2Ti_6O_{13}$ has been obtained using the $Na_2Ti_6O_{13}$ parent structure with a Li^+/Na^+ ion exchange method. Li-ion diffusion takes place through this [LiO_4] square-planar channel. Because of the abovementioned Li-ion coordination, $Li_2Ti_6O_{13}$ has been considered a 1D Li-ion conductor, similar to the case of ramsdellite $Li_2Ti_3O_7$. [7,10,12-15]

Computational methods are today an important complement to experiments in the study and design of materials. These techniques provide the means to precisely control the simulation

conditions, something which is difficult to truly achieve under experimental conditions. The use of theoretical design and simulation, with state-of-the-art first-principles approaches has been increasing, because it is an essential process for accelerating the discovery of new materials, which provides considerable accuracy of the structures and properties at the electronic level this calculation has been used in successful materials design efforts for applications as varied as alkali-ion batteries.[16,17] Atomistic simulations have been performed to disclose the main properties of materials. In particular $Li_2Ti_6O_{13}$, $Li_2Sn_6O_{13}$ structures [8] more recently, $Li_2Zr_6O_{13}$ emerged as a potential candidate electrode for Li-ion batteries.[8] The structural and electronic properties of these materials were studied in this article using density functional theory. The increase of the ionic radius of the B ions in the studied materials expands the unit cell parameters and the Li–Li distance in the channel of the $Li_2B_6O_{13}$ (B = Ti^{4+}, Sn^{4+}, or Zr^{4+}) compounds. Electronic structure calculations confirm that all structures present semiconductor characteristics. $Li_2Sn_6O_{13}$ presents the best semiconductor properties with a band gap of 1.24 eV. The open cell voltages are found to be 2.20, 2.70, and 1.95 V per Li^+/Li intercalation in $Li_2B_6O_{13}$ structures, respectively.[7,8] These predicted properties bring in new evidence to consider these $Li_2B_6O_{13}$ for use as alternative battery materials. The aim of this work consists of a theoretical exploration of structural and electronic properties of new compounds, namely $Na_2Zr_6O_{13}$ and $K_2Zr_6O_{13}$ as potential candidates as electrodes in alkali ion batteries.

Materials and methods

The compounds in concern are classified as 1D type structure $A_2Zr_6O_{13}$ (A= Li^+, $Na^{+,}$ and K^+), and exhibit large specific surface area and structural anisotropy.[8] The crystal structure of alkali hexazirconate $A_2Zr_6O_{13}$ with A = Li^+, $Na^{+,}$ or K^+ is shown in Figure 1. The $A_2Zr_6O_{13}$ consists of $[Zr_6O_{13}]^{-2}$ frameworks combined by alkali ions and oxygen in square planar hybridization. These properties are adopted from our assumption of the possible ion-exchange synthesis to obtain the $A_2Zr_6O_{13}$ from the known $A_2Ti_6O_{13}$ structures as follows:

$$A'_2Ti_6O_{13} + 6ZrO_2 \rightarrow A'_2Zr_6O_{13} + 6TiO_2 \qquad (1)$$

Once the $A'_2Zr_6O_{13}$ is derived from Equation (1) (e.g. with $A' = Li^+$), the following step considers the A' ion-exchange to obtain $Na_2Zr_6O_{13}$ and $K_2Zr_6O_{13}$ structures. The possibility of the abovementioned doubly ion-exchange reaction is justified because, in our previous works,

similar reactions were validated as a possible synthesis strategy for new compounds.[7, 18] In this concern, the $A_2Zr_6O_{13}$ are partners with each other, including their Ti-containing counterparts.

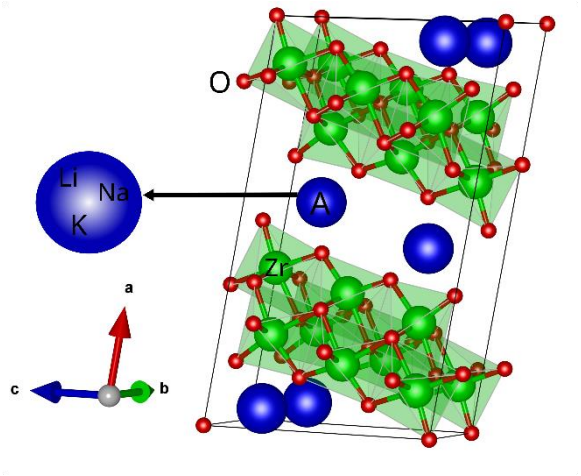

Fig. 1- Monoclinic $A_2Zr_6O_{13}$ (A= Li^+, Na^+ and K^+) in the conventional representation (*C*2/*m* space group). Blue red and green balls represent the A^+, $O^{2-,}$ and Zr^{4+} ions, respectively.

The experimental methods to find the improved negative electrodes for their use in high-performance batteries are expensive and slow mainly because they are based on trial-and-error procedures. DFT computations are used to predict the structural and electronic properties among other relevant magnitude concerning the development of battery materials.
DFT computations are performed to explore the structural and electronic properties of these structures. The CASTEP computer code was used to conduct the DFT calculations.[19] The generalized gradient approximation with Perdew-Burke-Ernzerhof formulation is used [20], together with the norm-conserving pseudopotentials (with a plane-wave energy cutoff of 750 eV) of A-ns^1, O-$2s^2$ $2p^4$ and Zr-$5s^2$ $5p^2$ electronic configuration is adopted. The convergence thresholds for self-consistent computations and geometry optimizations using a quasi-Newton algorithm to simultaneously relax the internal coordinates and lattice parameters of a crystal while preserving its symmetry are taken to be 10^{-6} eV/atom, with a maximum force of 10^{-3} eV/Å and stress and atomic displacements of 5×10^{-2} GPa and 5×10^{-4} Å, respectively.[21]
In this work, the monoclinic systems studied, $Na_2Zr_6O_{13}$ and $K_2Zr_6O_{13}$ have a conventional cell of 42 atoms with a space group of C2/m that we used for bulk calculations. For Na_2Zr6O_{13}, and $K_2Zr_6O_{13}$ the crystal structure is slightly modified (concerning those of $Li_2Zr_6O_{13}$) by shifting the Na/K atoms from Li positions in the fractional coordinate system. The crystal structures of $Na_2Zr_6O_{13}$ and $K_2Zr_6O_{13}$ are depicted in Figure 1. A Γ-centered

Monkhorst-Pack scheme is used to sample the Brillouin zone for geometry optimization. A k-point set of 7×7×3 along the reciprocal representation for the $A_2Zr_6O_{13}$ structures is used to obtain the total (DOS) and projected density of states (PDOS) in their reciprocal conventional representation.

Lattice static calculations, based on the force-field approach implemented in the GULP code [22], are also used to further explore the structural properties. Interatomic potential parameters (force-field) to model the ionic interactions are taken from the literature. Long–range interactions are treated by Coulombic forces while the short–range interactions are represented by Buckingham–type potentials. To complete the force field, the shell model is introduced to account for the ion polarization for the O–O interactions.[23] In the shell model, each ion is modeled as a positively charged core and negatively charged shell connected by a spring with a spring constant *k*. The sum of the core–shell charge is equal to the formal charge of each ion. To update the cell parameters and fractional positions of the equilibrium $A_2Zr_6O_{13}$ lattice structures, the Broyden–Fletcher–Goldfarb–Shanno (BFGS) approach is employed. These combinations of atomistic simulations have been widely used to provide accurate predictions regarding the relevant properties of ionic compounds.[7.23-25]

Results and discussion

Structural properties

The results of the cell parameters, obtained from DFT and classical force-field approaches, are compiled in Table 1. Small variations of the cell parameters derived by both methods are observed. For instance, the a- cell parameter increases progressively from $Li_2Zr_6O_{13}$ to $K_2Zr_6O_{13}$, which is attributed to the ionic radius difference between alkali ions. The *b*- cell parameter decreases slightly from 3.646 Å ($Li_2Zr_6O_{13}$) to 3.641 Å ($Na_2Zr_6O_{13}$) reaching its highest value in $K_2Zr_6O_{13}$ (3.684 Å). A similar variation in the *c*– cell parameter is observed, in which the Na^+/Li^+ ion-exchange induces no significant effect on the variation of *b*– and *c*– cell parameters. In the general case of $A_2B_6X_{13}$ ($B=Ti^{4+}$, Sn^{4+}, Zr^{4+}; $X = O^{2-}$, S^{2-}) structures, the shortest alkali jump distance coincides with the *b*– cell parameter.[8,25] This jump distance is of vital importance for the alkali migration within the [AO_4] channels through the $A_2Zr_6O_{13}$ lattice structures. In such an aspect, the $Li_2Zr_6O_{13}$ and $Na_2Zr_6O_{13}$ have similar jump distances. As shown in Table 1, the values of the structural parameters of $Li_2Zr_6O_{13}$ structures considered are consistent with those previously reported in the literature by DFT studies.[8] The cell parameters of all structures studied in this paper obtained by the use of the force field show a deviation of less than 10 % concerning the reported by DFT calculations.

The b variation concerning DFT calculation is more than 5 % contrary to other cell parameters that present small values. Our calculated cell parameters are also in line with the range previously reported in the literature.[8]

Table 1. Structural parameters of $A_2Zr_6O_{13}$ lattice structures in their C2/m conventional representation.

Structure		*a* (Å)	*b* (Å)	*c* (Å)	β (°)	Eg (eV)
	DFT	1,930	3,646	10,277	97,247	
$Li_2Zr_6O_{13}$	FF	16,548	3,909	9,858	97,498	3,788
	%	-2,31	6,72	-4,25	0,26	
	DFT	18,043	3,641	10,282	98,257	
$Na_2Zr_6O_{13}$	FF	17,413	3,922	9,857	98,998	3,474
	%	-3,62	7,18	-4,31	0,75	
	DFT	18,941	3,684	10,199	100,680	
$K_2Zr_6O_{13}$	FF	18,387	3,934	9,881	100,997	2,997
	%	-3,01	6,37	-3,22	0.31	

Electronic properties

Outstanding ionic-electronic properties are essential key requirements to consider compounds as electrodes. The band gap can be used to evaluate the electronic properties of a material.[8,26] The electronic band structures of $A_2Zr_6O_{13}$ are obtained using the same DFT setup. The total and projected density of states and band structures are obtained with the interpolation integration method with a broadening factor of 0.01 eV. Figure 2 displays the density of states (DOS), including the density of states of individual species of $Li_2Zr_6O_{13}$, $Na_2Zr_6O_{13,}$ and $K_2Zr_6O_{13}$ structures. In all samples, there is the accumulation of DOS near the Fermi level, characteristic of semiconductor materials. In all structures, Zr has a major contribution to the conduction band and O specie at the valence region. Alkali ions have less contribution to the electronic properties; in particular, K-ion has the major contribution to the conduction region reducing the energy band to 2.997 eV in $K_2Zr_6O_{13}$, as compared with the energy gap of ac. 3,788 and 3,474 eV for $Li_2Zr_6O_{13}$ and $Na_2Zr_6O_{13}$ compounds, respectively. The use of classical pseudopotentials in this paper provides a reliable approximation for ground state properties. However, their accuracy diminishes when estimating the band gap in semiconductors and insulator materials, potentially leading to an underestimation of up to

40%, depending on the specific material under investigation.[27] Additionally, for other hybrid functionals like HSE06, HSE03, and Hubbard approximations, the band gap value is dependent on additional parameters necessary to match experimental results. Given the absence of experimental data, we can only confidently determine the semiconductor or insulating nature of these materials. Furthermore, since K2Zr6O13, Na2Zr6O13, and Li2Zr6O13 are hypothetical compounds, combined with the aforementioned issue of DFT underestimating band gap calculations [7,18,28,29], the energy gap values presented in this study should be considered as lower bounds.

Together with the DOS analysis, Figure 3 shows the band structure of $Li_2Zr_6O_{13}$, $Na_2Zr_6O_{13}$, and $K_2Zr_6O_{13}$ computed in their ground state. The aforementioned insulating character of these compounds is confirmed by the presence of large energy bands near the Fermi level.

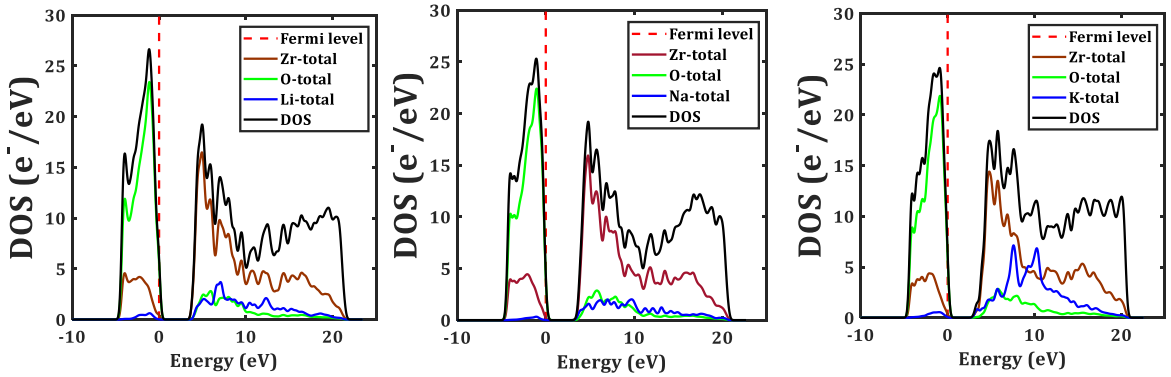

Fig. 2- The density of states of $Li_2Zr_6O_{13}$, $Na_2Zr_6O_{13}$, and $K_2Zr_6O_{13}$ structure, respectively. The vertical red line represents the Fermi level

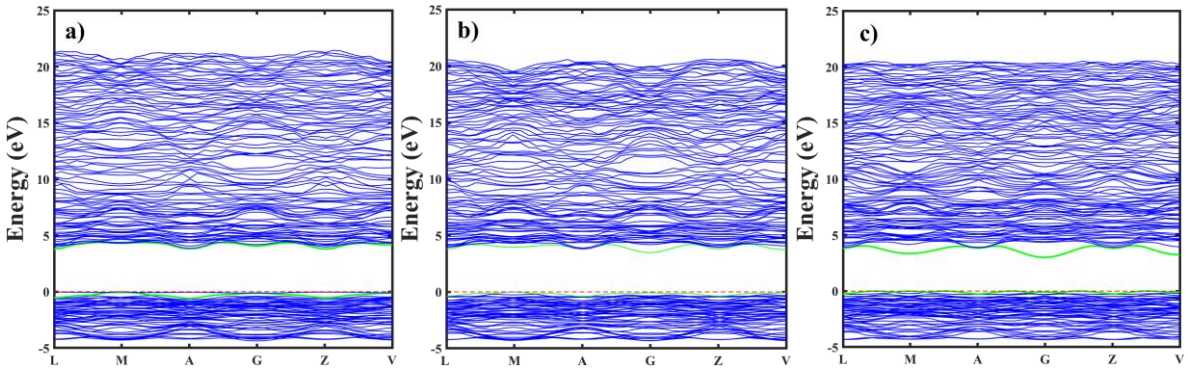

Fig. 3- Band structure profile of a) $Li_2Zr_6O_{13}$, b) $Na_2Zr_6O_{13}$, and c) $K_2Zr_6O_{13}$ compounds, respectively. The horizontal red line represents the Fermi level.

Thermodynamic analysis of $A_2Zr_6O_{13}$ formation via ion exchange reactions

Thermodynamic stability is a fundamental property of a material, providing quantitative information about the driving force for forming or decomposing a phase under equilibrium conditions. It is the principal quantity that suggests whether a compound can be formed and if it will persist under conditions of interest. First-principles calculations, such as those performed using DFT, have proven to be a reliable tool for determining thermodynamic stability for many known and newly proposed materials.[23,24,25,26,27,28,29,30]

However, it's important to note that while DFT for material stability considers isolated systems in vacuum at 0 K, the effect of temperature and other intensive properties can be captured in a thermodynamic stability analysis. In this case, it has been shown that formation energies are generally unaffected by this mapping from 0 K energies to 298 K enthalpies, due to cancellation of errors.[30]

The formation of the compounds under study can be evaluated by using the energy of possible reactions for the synthesis of the $A_2Zr_6O_{13}$, considering the energetics difference between reactants and product constituents. For instance, from Equation (1) we have: to obtain the $Li_2Zr_6O_{13}$ from the known Li2Ti6O13 structures as follows:

$$Li_2Ti_6O_{13} + 6ZrO_2 \rightarrow Li_2Zr_6O_{13} + 6TiO_2 \quad (2)$$

Once the $Li_2Zr_6O_{13}$ is derived, we can evaluate the alkali-ion exchange as follows:

$$Li_2Zr_6O_{13} + Na_2O \rightarrow Na_2Zr_6O_{13} + Li_2O \quad (3)$$

$$Li_2Zr_6O_{13} + K_2O \rightarrow K_2Zr_6O_{13} + Li_2O \quad (4)$$

$$K_2Zr_6O_{13} + Na_2O \rightarrow Na_2Zr_6O_{13} + K_2O \quad (5)$$

The reaction energy, ΔE_R, is then evaluated by:

$$\Delta E_R = \sum(E_{Products} - E_{Reactants}) \quad (6)$$

where

$E_{Products}$ and $E_{Reactants}$ represent the lattice energy of products and reactants, respectively, and the sums run over the product/reactant constituents.

While computational predictions of thermodynamic stability would ideally be directly related to synthesizability, the complex processes that can occur during synthesis are not purely thermodynamic (i.e., kinetics under difficult to describe conditions play a significant role) and today, cannot be easily captured with first-principles calculations.

The lattice energies of reactant and product constituents are computed by using the force field method adopting the same setup described in Section 2. Figure 4 b shows the possible reaction path to obtain the $A_2Zr_6O_{13}$ compounds. The sums of the energy of reactants and products were calibrated as a baseline to help the view as shown in the Figure 4 a. The results show that the formation of $Na_2Zr_6O_{13}$ from $Li_2Zr_6O_{13}$, described by Equation (3), is less thermodynamical unfavourable with ΔE_R of -1,21 eV, followed by the formation of $Li_2Zr_6O_{13}$ [Equation (2)] with -1,08 eV. The formation of $Na_2Zr_6O_{13}$ [Equation (5)] with ΔE_R of -0, 52 eV is the most thermodynamical favourable, followed by the formation of $K_2Zr_6O_{13}$ [Equation (4)] with an energetics cost of ac. -0, 69 eV, respectively.

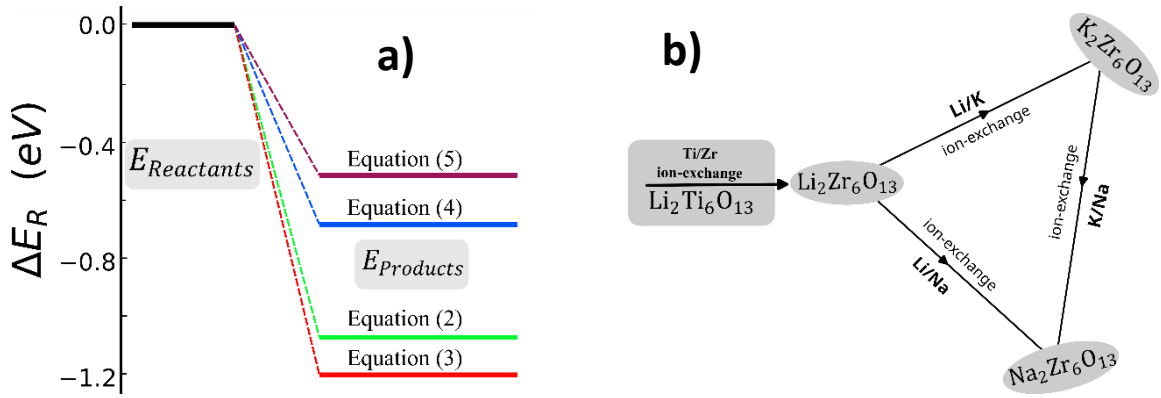

Fig. 4- a) Reaction energy of hypothetical $A_2Zr_6O_{13}$ synthesis, b) Hypothetical reaction path to obtain these compounds by ion exchange synthesis

In previous works, concerning computational material design of $Li_2B_6X_{13}$ (A = Li^+, Na^+, K^+; B =Ti^{4+}, Sn^{4+}; X = O^{2-}, S^{2-}), we demonstrated the possibility of the Sn^{4+}/Ti^{4+} ion-exchange to form evaluating their decomposition energy.[7-9,18,28] But only are thermodynamically favourable the ion exchange reaction showed in Figure 4 b.

Conclusions

In this study, the structural, electronic, and mechanical properties of $Li_2Zr_6O_{13}$, as well as the previously unreported compounds $Na_2Zr_6O_{13}$ and $K_2Zr_6O_{13}$, were comprehensively assessed through classical simulations and Density Functional Theory (DFT) calculations. The structural properties were determined using force-field methods, and their accuracy was subsequently verified via DFT computations. The lattice parameters obtained through DFT calculations closely align with prior research findings, which utilized GGA PBE functionals and the force field methodology. This underscores the capability of the force field approach to effectively model such materials, facilitating extensive exploration for novel and intriguing compounds. The electronic band structure analysis indicates that $Li_2Zr_6O_{13}$ and $Na_2Zr_6O_{13}$ exhibit insulator behavior, featuring indirect band gap energies of 3,788 eV and 3,474 eV, respectively. In contrast, $K_2Zr_6O_{13}$ demonstrates semiconducting properties with a band gap energy of 2,997 eV. Our research substantiates the feasibility of ion exchange reactions involving Li/K, Li/Na, and K/Na, proving their energy-efficient potential in synthesizing the previously unidentified materials $K_2Zr_6O_{13}$ and $Na_2Zr_6O_{13}$. In summary, hexazirconates of potassium and sodium can be efficiently synthesized through ion exchange reactions, making them promising candidates for energy storage applications in ion batteries.

Acknowledgments

This project received support from the Flemish Development Cooperation through the Flemish Interuniversity Council-University Cooperation for Development (VLIR-UOS) as part of an Institutional University Cooperation program with Universidad de Oriente in Santiago de Cuba, Cuba.

FT wishes to acknowledge the VUB for support, among other through a Strategic Research Program awarded to his group. Computational resources and services were provided by the Shared ICT Services Centre funded by the Vrije Universiteit Brussel, the Flemish Supercomputer Center (VSC) and FWO.

Reference

1. Saiful Islam, M.; J. Fisher, C. A. Lithium and Sodium Battery Cathode Materials: Computational Insights into Voltage, Diffusion and Nanostructural Properties. *Chemical Society Reviews* **2014**, *43* (1), 185–204. https://doi.org/10.1039/C3CS60199D.
2. Whittingham, M. S. Lithium Batteries and Cathode Materials. *Chem. Rev.* **2004**, *104* (10), 4271–4302. https://doi.org/10.1021/cr020731c.
3. Ellis, B. L.; Lee, K. T.; Nazar, L. F. Positive Electrode Materials for Li-Ion and Li-Batteries †. *Chem. Mater.* **2010**, *22* (3), 691–714. https://doi.org/10.1021/cm902696j.
4. Deng, D. Li-Ion Batteries: Basics, Progress, and Challenges. *Energy Sci Eng* **2015**, *3* (5), 385–418. https://doi.org/10.1002/ese3.95.
5. Andersson, S.; Wadsley, A. D. The Structures of $Na_2Ti_6O_{13}$ and $Rb_2Ti_6O_{13}$ and the Alkali Metal Titanates. *Acta Crystallographica* **1962**, *15* (3), 194–201. https://doi.org/10.1107/S0365110X62000511.
6. Dominko, R.; Dupont, L.; Gaberšček, M.; Jamnik, J.; Baudrin, E. Alkali Hexatitanates—$A_2Ti_6O_{13}$ (A=Na, K) as Host Structure for Reversible Lithium Insertion. *Journal of Power Sources* **2007**, *174* (2), 1172–1176. https://doi.org/10.1016/j.jpowsour.2007.06.181.
7. Zulueta, Y. A.; Geerlings, P.; Tielens, F.; Nguyen, M. T. Lithium- and Sodium-Ion Transport Properties of $Li_2Ti_6O_{13}$, $Na_2Ti_6O_{13}$ and $Li_2Sn_6O_{13}$. *Journal of Solid State Chemistry* **2019**, *279*, 120930. https://doi.org/10.1016/j.jssc.2019.120930.
8. Fernández-Gamboa, J. R.; Tielens, F.; Zulueta, Y. A. Theoretical Study of $Li_2Ti_6O_{13}$, $Li_2Sn_6O_{13}$ and $Li_2Zr_6O_{13}$ as Possible Cathode in Li-Ion Batteries. *Materials Science in Semiconductor Processing* **2022**, *152*, 107074. https://doi.org/10.1016/j.mssp.2022.107074.
9. Simalaotao, K.; Thanasarnsurapong, T.; Maluangnont, T.; Phacheerak, K.; Boonchun, A. Elastic Properties of $A_2Ti_6O_{13}$ (H, Li, Na, K and Rb): A Computational Study. *J. Phys. D: Appl. Phys.* **2023**, *56* (38), 385303. https://doi.org/10.1088/1361-6463/acd790.
10. Kataoka, K.; Awaka, J.; Kijima, N.; Hayakawa, H.; Ohshima, K.; Akimoto, J. Ion-Exchange Synthesis, Crystal Structure, and Electrochemical Properties of $Li_2Ti_6O_{13}$. *Chem. Mater.* **2011**, *23* (9), 2344–2352. https://doi.org/10.1021/cm103678e.
11. Peréz-Flores, J. C.; Kuhn, A.; Alvarado, F. G.-. A Comparative Electrochemical Study of $Li_2Ti_6O_{13}$ and $Na_2Ti_6O_{13}$. *Meet. Abstr.* **2010**, *MA2010-03* (1), 280. https://doi.org/10.1149/MA2010-03/1/280.

12. Flores, J. C. P.; Hoelzel, M.; Kuhn, A.; Alvarado, F. G. On the Mechanism of Lithium Insertion into $A_2Ti_6O_{13}$ (A = Na, Li). *ECS Trans.* **2012**, *41* (41), 195. https://doi.org/10.1149/1.4717977.
13. Pérez-Flores, J. C.; Kuhn, A.; García-Alvarado, F. Synthesis, Structure and Electrochemical Li Insertion Behaviour of $Li_2Ti_6O_{13}$ with the $Na_2Ti_6O_{13}$ Tunnel-Structure. *Journal of Power Sources* **2011**, *196* (3), 1378–1385. https://doi.org/10.1016/j.jpowsour.2010.08.106.
14. Pérez-Flores, C. J.; Kuhn, A.; García-Alvarado, F. A Structural and Electrochemical Study of $Li_2Ti_6O_{13}$. *MRS Online Proceedings Library* **2011**, *1313* (1), 8. https://doi.org/10.1557/opl.2011.1390.
15. Pérez-Flores, J. C.; Baehtz, C.; Hoelzel, M.; Kuhn, A.; García-Alvarado, F. Full Structural and Electrochemical Characterization of Li2Ti6O13 as Anode for Li-Ion Batteries. *Phys. Chem. Chem. Phys.* **2012**, *14* (8), 2892. https://doi.org/10.1039/c2cp23741e.
16. Kraytsberg, A.; Ein-Eli, Y. Higher, Stronger, Better… A Review of 5 Volt Cathode Materials for Advanced Lithium-Ion Batteries. *Advanced Energy Materials* **2012**, *2* (8), 922–939. https://doi.org/10.1002/aenm.201200068.
17. Van der Ven, A.; Deng, Z.; Banerjee, S.; Ong, S. P. Rechargeable Alkali-Ion Battery Materials: Theory and Computation. *Chem. Rev.* **2020**, *120* (14), 6977–7019. https://doi.org/10.1021/acs.chemrev.9b00601.
18. Zulueta, Y. A.; Nguyen, M. T. Lithium Hexastannate: A Potential Material for Energy Storage. *physica status solidi (b)* **2018**, *255* (7), 1700669. https://doi.org/10.1002/pssb.201700669.
19. Clark, S. J.; Segall, M. D.; Pickard, C. J.; Hasnip, P. J.; Probert, M. I. J.; Refson, K.; Payne, M. C. First Principles Methods Using CASTEP. *Zeitschrift für Kristallographie - Crystalline Materials* **2005**, *220* (5–6), 567–570. https://doi.org/10.1524/zkri.220.5.567.65075.
20. Perdew, J. P.; Ruzsinszky, A.; Csonka, G. I.; Vydrov, O. A.; Scuseria, G. E.; Constantin, L. A.; Zhou, X.; Burke, K. Restoring the Density-Gradient Expansion for Exchange in Solids and Surfaces. *Phys. Rev. Lett.* **2008**, *100* (13), 136406. https://doi.org/10.1103/PhysRevLett.100.136406.
21. Pfrommer, B. G.; Côté, M.; Louie, S. G.; Cohen, M. L. Relaxation of Crystals with the Quasi-Newton Method. *Journal of Computational Physics* **1997**, *131* (1), 233–240. https://doi.org/10.1006/jcph.1996.5612.

22. D. Gale, J. GULP: A Computer Program for the Symmetry-Adapted Simulation of Solids. *Journal of the Chemical Society, Faraday Transactions* **1997**, *93* (4), 629–637. https://doi.org/10.1039/A606455H.
23. Zulueta, Y. A.; Dawson, J. A.; Froeyen, M.; Nguyen, M. T. Structural Properties and Mechanical Stability of Monoclinic Lithium Disilicate: Structural Properties of Monoclinic Lithium Disilicate. *Phys. Status Solidi B* **2017**, *254* (10), 1700108. https://doi.org/10.1002/pssb.201700108.
24. Zulueta, Y. A.; Froeyen, M.; Nguyen, M. T. Structural Properties and Mechanical Stability of Lithium-Ion Based Materials. A Theoretical Study. *Computational Materials Science* **2017**, *136*, 271–279. https://doi.org/10.1016/j.commatsci.2017.04.033.
25. Zulueta, Y. A.; Geerlings, P.; Tielens, F.; Nguyen, M. T. Influence of Oxygen–Sulfur Exchange on the Structural, Electronic, and Stability Properties of Alkali Hexastannates. *J. Phys. Chem. C* **2019**, *123* (40), 24375–24382. https://doi.org/10.1021/acs.jpcc.9b06295.
26. Schlüter, M.; Sham, L. J. Density-Functional Theory of the Band Gap. In *Advances in Quantum Chemistry*; Löwdin, P.-O., Ed.; Density Functional Theory of Many-Fermion Systems; Academic Press, 1990; Vol. 21, pp 97–112. https://doi.org/10.1016/S0065-3276(08)60593-6.
27. Perdew, J. P. Density Functional Theory and the Band Gap Problem. *Int. J. Quantum Chem.* **2009**, *28* (S19), 497–523. https://doi.org/10.1002/qua.560280846.
28. Zulueta Leyva, Y. A.; Nguyen, M. T. Implications of Oxygen–Sulfur Exchange on Structural, Electronic Properties, and Stability of Alkali-Metal Hexatitanates. *Phys. Status Solidi B* **2019**, *256* (8), 1800568. https://doi.org/10.1002/pssb.201800568.
29. Medvedev, M. G.; Bushmarinov, I. S.; Sun, J.; Perdew, J. P.; Lyssenko, K. A. Density Functional Theory Is Straying from the Path toward the Exact Functional. *Science* **2017**, *355* (6320), 49–52. https://doi.org/10.1126/science.aah5975.
30. Bartel, C. J. Review of Computational Approaches to Predict the Thermodynamic Stability of Inorganic Solids. *J Mater Sci* **2022**, *57* (23), 10475–10498. https://doi.org/10.1007/s10853-022-06915-4.

Conflict of interest

The authors declare no conflict of interest.

Author contributions

J.R. Fernández-Gamboa performed the quantum mechanical calculations, implemented the computational models, and analyzed the ab initio simulation data. They were responsible for running the simulations and obtaining the results presented in the paper.

Yohandys A. Zulueta and **Frederick Tielens** conceived and designed the research, providing the overall guidance and project management.

My Phuong Pham-Ho and **Minh Tho Nguyen** all authors contributed to the writing, reviewing, and editing of the final version.